# Establishment of Porcine and Human Expanded Potential Stem Cells

Xuefei Gao[1,2*], Monika Nowak-Imialek[3*], Xi Chen[2*], Dongsheng Chen[4], Degong Ruan[5], Melanie A. Eckersley-Maslin[6], Ahmad Shakil[7], Toshihiro Kobayashi[8], Guocheng Lan[9], David Ryan[2], Stoyan Petkov[3], Jian Yang[2], Liliana Antunes[2], Lia S. Campos[2], Fengtang Yang[2], Beiyuan Fu[2], Shengpeng Wang[4], Yong, Yu[2], Xiaomin Wang[5], Song-Guo Xue[10], Liangpeng Ge[11], Zuohua Liu[11], Yong Huang[11], Tao Nie[5], Donghai Wu[5], Duanqing Pei[5], Yi Zhang[12], Liming Lu[13], Susan. J. Kimber[14], Wolf Reik[6], Xiangang Zou[9], Patrick P. L. Tam[15], Ahmed Asif[7], Azim Surani[8], Liangxue Lai[5], Zhouchun Shang[4], Sarah A. Teichmann[2], Heiner Niemann[3], Pentao Liu[1,2]

1. The University of Hong Kong, Li Ka Shing Faculty of Medicine, School of Biomedical Sciences, Stem cell and regenerative medicine consortium, 5 Sassoon Road, Pokfulam, Hong Kong
2. The Wellcome Sanger Institute, Wellcome Genome Campus, Hinxton, Cambridge, CB10 1HH, UK
3. Institute of Farm Animal Genetics, Friedrich-Loeffler-Institut (FLI), Mariensee, 31535 Neustadt, Germany and REBIRTH, Centre of Excellence, Hannover Medical School, 30625 Hannover, Germany
4. BGI-Shenzhen, Shenzhen 518083 China, and China National GeneBank, BGI-Shenzhen, Shenzhen 518120, China.
5. Key Laboratory of Regenerative Biology, Guangzhou Institutes of Biomedicine and Health, Chinese Academy of Sciences, 510530 Guangzhou, China
6. Epigenetics Programme, Babraham Institute, Babraham Research Campus, Cambridge, CB22 3AT, UK
7. Aston Medical School, Aston University, Birmingham B4 7ET, UK
8. Wellcome Trust and Cancer Research UK Gurdon Institute, University of Cambridge, Tennis Court Road, Cambridge CB2 1QN, UK
9. Cancer Research UK Cambridge Institute, University of Cambridge, Cambridge, CB2 0RE, UK
10. Center for Reproductive Medicine, Shanghai East Hospital, Tong Ji University School of Medicine. Shanghai 200120 China
11. Chongqing Academy of Animal Sciences, and Key Laboratory of Pig Industry Sciences, Department of Agriculture, Chongqing, 402460, China
12. Zhengzhou University first affiliated Hospital, Henan, China
13. Institute of Immunology, Shanghai Jiaotong University School of Medicine, Shanghai 200025, China
14. Faculty of Biology Medicine and Health, University of Manchester, Oxford Road, Manchester M13 9PT, U. K
15. Embryology Unit, Children's Medical Research Institute and School of Medical Sciences, Sydney Medical School, Faculty of Medicine and Health, The University of Sydney, Westmead, NSW 2145, Australia

*Equal contribution

[§]Correspondence should be addressed to:

Pentao Liu, Ph.D. E-mail: pliu88@hku.hk or

Heiner Niemann, Ph.D. E-mail: heiner.niemann@fli.de

We recently derived pluripotent stem cells with an expanded potency for both extraembryonic and embryonic cell lineages (EPSCs) from individual blastomeres by inhibiting the activity of critical molecular pathways that predisposes lineage differentiation in the mouse preimplantation embryo [1]. We now report the derivation of porcine EPSC (pEPSC) lines either directly from preimplantation embryos or by reprogramming fetal fibroblasts. The pEPSCs express key pluripotency genes, contribute to both trophoblast and embryonic tissues in the chimeras, and produce primordial germ cell-like cells (PGCLCs) *in vitro*. Under similar culture conditions, human ESCs and iPSCs can be converted or somatic cells directly reprogrammed to EPSCs (hEPSCs) that display the molecular and functional attributes reminiscent of pEPSCs and human 8-cell and morula stage embryos. Significantly, trophoblast stem cells can be generated from both human and porcine EPSCs. Our pathway-inhibition paradigm opens a new avenue for isolating EPSCs in mammalian species in which pluripotent embryonic stem cells are yet to be established. These stem cells, which are proximal to the totipotency state, present new opportunities for translational research in biotechnology and regenerative medicine.

Key words: embryonic stem cells, preimplantation embryos, porcine, chimeras, human, germ cells, trophoblast, placenta, single cell RNA sequencing, histone methylation, DNA methylation, developmental potential, totipotency

To this date, *bona fide* pluripotent stem cells have yet to be established from preimplantation porcine embryos [2-9]. We have recently demonstrated that by targeting key molecular pathways that drive lineage differentiation in the preimplantation embryo, mouse expanded potential stem cells (mEPSCs) displaying a broad propensity for extraembryonic and embryonic lineage differentiation can successfully be derived [1]. We hypothesized that a similar experimental paradigm of targeting key developmental pathways could be applied for establishing pluripotent stem cell lines from porcine preimplantation embryos. Since little is known about the molecular and signalling mechanisms of porcine early preimplantation embryo development, we elected to perform a chemical screen of inhibitors that were used for isolating and maintaining mouse ESCs, mEPSCs and human ESCs to delineate the optimal condition for pig pluripotent stem cells. While porcine iPSCs are available, the use of these cells for the screen is confounded by the leaky expression of transgenic reprogramming factors after reprogramming or low levels of expression of endogenous pluripotency genes [10-18]. To overcome this challenge, we generated new porcine iPSCs that expressed Doxycycline (Dox)-inducible *LIN28*, *NANOG*, *LRH1* and *RARG*, in concert with the four Yamanaka factors. This strategy substantially improved the efficiency of reprogramming wild-type German Landrace porcine fetal fibroblasts (PFFs) and transgenic PFFs, in which a *tdTomato* cassette had been inserted into the 3' UTR of the porcine *OCT4* (*POU5F1*) locus (POT PFFs) [19], to putative iPSC colonies (Extended Data Fig. 1a-c). The reprogrammed primary colonies from POT PFFs were OCT4-tdTomato$^{+}$, indicating the re-activation of the *OCT4* locus (Extended Data Fig. 1c). Indeed, the iPSCs expressed high levels of the endogenous pluripotency factors revealed by RT-qPCR (Extended Data Fig. 1d), and could be passaged as single cells for more than 20 passages in serum-containing

92 medium (M15) plus Dox. Upon Dox removal, the iPSCs differentiated within 4-5
93 days, concomitant with the rapid down-regulation of the exogenous reprogramming
94 factors and endogenous pluripotency genes and with the increased expression of both
95 embryonic and extraembryonic cell lineage genes (Extended Data Fig. 1e-h). These
96 Dox-dependent porcine iPSCs with robust endogenous pluripotency gene expression
97 provided the material for the chemical screen.

98 In the screen, over 400 combinations of 20 small molecule inhibitors and cytokines
99 were tested in their ability to maintain Dox-independent pig iPSCs in the
100 undifferentiated state (Extended Data Fig. 2a; Supplementary Table 1). A departure
101 was noted from previous reports that naïve mouse ESC medium 2i/LIF was able to
102 maintain putative pig iPSCs [14, 16, 20]: pig iPSCs were rapidly lost in the presence
103 of Mek1 inhibitor PD-0325901, irrespective of whether Dox was present or not
104 (Extended Data Fig. 2b-h), indicating that a certain level of Mek-ERK signalling
105 would be vital for pig pluripotent stem cells. Inhibition of p38 and PKC was also non-
106 conducive for pig iPSCs (Extended Data Fig. 2b-h and Extended Data Fig. 3a). These
107 findings led us to conclude that mouse or human naïve ESC conditions [21-23] cannot
108 be directly extrapolated to pig pluripotent stem cells, and these three inhibitors were
109 therefore excluded from the screen. Our work identified several conditions (Extended
110 Data Fig. 2h), including a minimal requisite condition (#517, pig EPSC medium:
111 pEPSCM) comprising inhibitors for GSK3 (CHIR99021), SRC (WH-4-023) and
112 Tankyrases (XAV939) (the last two were inhibitors important for mouse EPSCs[1]),
113 and supplements: Vitamin C (Vc), ACTIVIN A and LIF (Extended Data Fig. 2a, 2h
114 and Supplementary Table 1). Under this condition, the Dox-independent iPSCs
115 ($pEPSC^{iPS}$) remained undifferentiated in 30 passages, expressed endogenous

pluripotency factors at levels comparable to the porcine blastocyst and showed no leaky expression of the exogenous reprogramming factors (Extended Data Fig. 3b-d).

We next repeated the PFF reprogramming experiment by directly culturing the primary colonies in pEPSCM (Extended Data Fig. 3e), and generated 11 stable pEPSC$^{iPS}$ lines from 16 primary colonies (70% efficiency). All lines expressed high levels of endogenous pluripotency genes and six of them did not have detectable expression of any of the eight exogenous reprogramming factors (Extended Data Fig. 3f). We next employed this pEPSCM condition to derive stem cell lines directly from pig preimplantation embryos. A total of 26 lines (pEPSCs$^{Emb}$, 14 male and 12 female) were established from 76 early blastocysts (5.0 dpc), and 12 cell lines (pEPSCs$^{par}$) from 252 parthenogenetic blastocysts (Fig. 1a, Table 1 and Extended Data Fig. 3g). Like the pEPSCs$^{iPS}$, pEPSCs$^{Emb}$ had high nuclear/cytoplasmic ratios, formed compact colonies with smooth colony edges (Fig. 1a, Extended Data Fig. 3h). The pEPSCs$^{Emb}$ were passaged every 3-4 days at 1:10 ratio as single cells and could be maintained for >40 passages without overt differentiation. Subcloning efficiency was about 10% at low cell density (2,000 cells per well in 6-well plate), but high cell densities were always used in routine passaging. pEPSCs$^{Emb}$ were karyotypically normal after 25 passages (Extended Data Fig. 4a).

The pEPSCs$^{Emb}$ and pEPSC$^{iPS}$ expressed pluripotency genes at comparable levels as the blastocysts (Extended Data Fig. 3f), which were verified by immunostaining (Extended Data Fig. 4b). They showed extensive DNA demethylation at the *OCT4* and *NANOG* promoter regions (Fig. 1b), had *OCT4* distal enhancer activity (Extended Data Fig. 4c). The EPSCs were amenable for Crispr/Cas9-mediated insertion of a *H2B-mCherry* expression cassette into the *ROSA26* locus (Extended Data Fig. 4d and 4e). *In vitro*, pEPSCs differentiated to tissues expressing the markers of three germ

layers: SOX7, AFP, T, DES, CRABP2, SMA, β-Tubulin and PAX6 and, uniquely, the trophoblast markers HAND1, GATA3, PGF and KRT7 (Fig. 1c, Extended Data Fig. 4f). In immunocompromised mice, pEPSCs$^{Emb}$ formed mature teratomas containing derivatives of the three germ layers and placental lactogen-1 positive (PL-1$^{+}$) trophoblast-like cells (Fig. 1d and 1e). These results indicate that pEPSCs$^{Emb}$ and pEPSCs$^{iPS}$, like mEPSCs [1], may possess an expanded differentiation potential for both the embryonic and extra-embryonic trophoblast lineages. The pEPSCs were tested for their contribution to blastocyst cell lineages in chimeras. Following incorporation of the pEPSCs into preimplantation embryos and after 48 hours of culture, pEPSCs (marked by EF1a-H2B-mCherry) had colonized both the trophectoderm and inner cell mass of the blastocyst (Extended Data Fig. 5a). Following the transfer of the chimeric embryos to pseudo-pregnant recipient sows, a total of 45 conceptuses were harvested from 3 litters at days 26-28 of gestation (Supplementary Table 2, Extended Data Fig. 5b). Flow cytometry of single cells collected from the embryonic and extraembryonic tissues of the chimeras revealed the presence of mCherry$^{+}$ cells in 7 conceptuses (Extended Data Fig. 5c, Supplementary Table 3 and 4): mCherry$^{+}$ cells in both the placenta and embryonic tissues in 2 chimeras (#8 and #16); only in embryonic tissues of 3 chimeras (#4, #21 and #34); and exclusively in the placenta of 2 chimeras (#3 and #6). Genomic DNA PCR assays detected mCherry DNA only in those seven mCherry$^{+}$ chimeras, but not in any other conceptuses (Extended Data Fig. 5d, Supplementary Table 3 and 4). Despite the overall low contribution from the donor mCherry$^{+}$ cells, they were found in multiple host embryonic tissues and organs and expressed the appropriate tissue lineage markers: SOX2, TUJ1, GATA4, SOX17, AFP and α-SMA (Fig. 1f-g and Extended

Data Fig. 5e-f). In placental cells, mCherry was co-detected with the trophoblast markers PL-1 and KRT7 (Extended Data Fig. 5f).

We next tested if pEPSCs had the potential to produce PGC-like cells (PGCLCs) *in vitro,* similar to mouse and human pluripotent stem cells [24-26]. In early-primitive streak (PS)-stage pig embryos (E11.5–E12), the first cluster of pig PGCs can be detected as $SOX17^+$ cells in the posterior end of the nascent primitive streak, and these cells later co-express OCT4, NANOG, BLIMP1 and TFAP2C [25]. *NANOS3* is an evolutionarily conserved PGC-specific factor [27, 28] and human *NANOS3* reporter cells have been used for studying PGCLCs from pluripotent stem cells [25, 26]. To facilitate identification of putative pig PGCLCs, we targeted the *H2B-mCherry* reporter cassette to the 3' UTR of the *NANOS3* locus in $pEPSCs^{Emb}$ (Line K3, male) (Extended Data Fig. 6a). After expressing the *SOX17* transgene transiently for 12 hours, the *NANOS3* reporter $pEPSCs^{Emb}$ were allowed to form embryoid bodies (EBs) (Extended Data Fig. 6b), which generated cell clusters co-expressing *NANOS3* ($mCherry^+$) and tissue-nonspecific alkaline phosphatase (TNAP, a PGC marker) in 3-4 days (Fig. 2a).

The derivation of putative pig PGCLCs was BMP2/4 dependent, as removal of BMP2 from the EB culture or inhibition of the BMP2/4 signaling by inhibitor LDN-193189 abrogated the formation of $mCherry^+/TNAP^+$ cell clusters (Fig. 2a). Expressing *NANOG*, *BLIMP1* or *TFAP2C* transgenes in pEPSCs, either individually or in combinations, had no effect on the preponderance of $NANOS3^+$ cells (Extended Data Fig. 6c), which was different from the reported derivation of human PGCLCs [25]. However, co-expression of *SOX17* with *BLIMP1,* but not *NANOG* or *TFAP2C*, increased the population of $NANOS3^+$ cells (Extended Data Fig. 6c).

The mCherry$^{+}$ (*NANOS3*$^{+}$) putative PGCLCs in the EBs expressed PGC genes *NANOS3*, *BLIMP1*, *TFAP2C*, *CD38*, *DND1*, *KIT* and *OCT4* [25], which was detected in RT-qPCR and was confirmed in immunofluorescence at single cell resolution (Fig. 2b-c, and Extended Data Fig. 6d). Specific RNA-seq analysis of the mCherry$^{+}$/*NANOS3*$^{+}$ cells revealed expression of early PGC genes (*OCT4*, *NANOG*, *LIN28A*, *TFAP2C*, *CD38*, *DND1*, *NANOS3*, *ITGB3*, *SOX15* and *KIT*), and reduced *SOX2* expression (Fig. 2d-e, Supplementary Table 5) [26]. During the PGC derivation from human ESCs, cells undergo global DNA demethylation, which is accompanied by upregulation of TETs and down-regulation of DNMT3A/B [26]. Similarly, relative to the parental pEPSCs$^{Emb}$, *DNMT3B* was down-regulated in pig mCherry$^{+}$/*NANOS3*$^{+}$ cells, whereas *TET1/2* were up-regulated (Fig. 2e-f, Supplementary Table 5).

The findings that inhibition of SRC and Tankyrases is sufficient to convert mouse ESCs to mEPSCs [1] and that the same two inhibitors are required for the generation of pEPSCs raise the possibility that similar *in vitro* culture conditions may also work for deriving and maintaining EPSCs of other mammalian species. Four established human ES cell (hESC) lines (H1, H9, M1 and M10 cells) were cultured in pEPSCM and passaged up to three times. The cells displayed diverse morphologies and heterogeneous expression of OCT4 (Extended Data Fig. 7a). Removing ACTIVIN A (20ng/ml) from pEPSCM led to fewer cell colonies derived from H1 (<1.0%) and M1 (5.0%) ESC lines, and none from H9 or M10 (Extended Data Fig. 7a), an observation consistent with the inherent between-line heterogeneity of human ESCs [29, 30]. With further refinement of the culture condition (For example, replacing A-419259 with another SRC inhibitor WH-4-023 in hEPSCM, see Methods), morphologically homogenous and stable cell lines were established from single-cell sub-cloned H1 (H1-EPSCs) and M1 cells (M1-EPSCs) (Fig. 3a). Karyotype analysis of H1 and M1

cells grown in hEPSCM revealed genetic stability (at passage 25, Extended Data Fig. 7b). When human primary iPSC colonies reprogrammed by the six-factor system [31] were directly cultured in hEPSCM, around 70% picked colonies could be established into stable iPSC lines (iPSC-EPSCs). (Extended Data Fig. 7c). These iPSCs expressed pluripotency markers with no obvious leakiness of the exogenous reprogramming factors (Extended Data Fig. 7d-e). The H1-EPSCs proliferated more robustly than the H1 ESCs cultured in standard FGF-containing medium (H1-ESC) or in the naïve 5i/L/A conditions (H1-naïve ESC) [21] (Extended Data Fig. 7f), and were tolerant of single cell passaging with a 10% single cell sub-cloning efficiency in the transient presence of ROCKi. Cell survival at passaging was substantially improved in the presence of 5.0ng/ml ACTIVIN A or by splitting the cells at higher density. Human EPSCs expressed pluripotency genes (*OCT4*, *SOX2*, *NANOG*, *REX1* and *SALL4*) at higher levels than the H1-ESCs (Extended Data Fig. 7d) but minimal levels of lineage markers (*EOMES*, *GATA4*, *GATA6*, *T*, *SOX17* and *RUNX1*) (Extended Data Fig. 7g). Expression of core pluripotency factors and surface markers in human EPSCs was confirmed by immunostaining (Extended Data Fig. 7h). H1-EPSCs differentiated to derivatives of the three somatic germ layers *in vitro* and *in vivo* (Extended Data Fig. 7i-j). Moreover, H1-EPSCs were successfully differentiated to PGCLCs using the *in vitro* conditions developed for germ cell competent hESCs or iPSCs [25, 26] (Extended Data Fig. 7k-l).

Our results demonstrate that human and pig EPSCs could be derived and maintained using the similar set of small molecule inhibitors. Global gene expression profiling revealed that pEPSCs and hEPSCs clustered together, but were distinct from human primed ESCs or PFFs [1, 21] (Fig. 3b, Extended Data Fig. 8a and Supplementary Table 6-7). Both pig and human EPSCs expressed high levels of key pluripotency

239 genes, low levels of the somatic cell lineage genes, *SOX1*, *PAX6*, *T*, *GATA4* and
240 *SOX7*, and in general placenta-related genes such as *PGF*, *TFAP2C*, *EGFR*, *SDC1*
241 and *ITGA5* (Extended Data Fig. 8b-c). Consistent with the high level of global DNA
242 methylation of pEPSCs and hEPSCs (Extended Data Fig. 8d), DNA methyltransferase
243 genes *DNMT1* and *DNMT3A* and *DNMT3B* were highly expressed, whereas *TET1*,
244 *TET2* and *TET3* expressed at lower levels (Extended Data Fig. 8e). Among the highly
245 expressed 76 genes (>8-fold increase) in H1-EPSC in comparison to H1-ESCs, 17
246 genes encode histone variants with 15 belonging to the histone cluster 1 (Fig. 3c and
247 Supplementary Table 8). Interestingly, these histone genes were expressed at low
248 levels in 5i and primed human ESCs but were highly expressed in human 8-cell and
249 morula stage embryos (Fig. 3d). These histone genes were also discovered to be
250 expressed at significantly higher levels in additional hEPSC lines when compared
251 with the same cells cultured either in the conventional human ESC medium (FGF) or
252 5i (naïve) medium (Fig. 3e). The biological significance of high histone gene
253 expression in hEPSCs and in human 8-cell and morula embryos remains to be
254 explored. Single cell RNA-seq (scRNAseq) of pig and human EPSCs revealed
255 uniform expression of the core pluripotency factors: *OCT4*, *SOX2*, *NANOG* and
256 *SALL4* (Fig. 3f), and substantially homogenous cell cultures (Fig. 3g). At the single-
257 cell level, mouse EPSCs were enriched for transcriptome of 4-cell to 8-cell
258 blastomeres [1], whereas hEPSCs were more similar to human 8-cell to morula stage
259 embryos [32, 33] (Fig. 3h, and Extended Data Figure 8f), which is in line with the
260 histone gene expression profiles (Fig. 3d). Interestingly, transcriptome analysis also
261 revealed low expression levels of naïve pluripotency factors such as *KLF2* in EPSCs
262 (Fig. 3f and Extended Data Fig. 8b), which is not expressed in human early
263 preimplantation embryos [34]. Although *KLF2*, *TET1*, *TET2* and *TET3* were weakly

expressed in EPSCs (Extended Data Fig. 8b), their promoter regions were decorated with active H3K4m3 histone marks (Extended Data Fig. 8g). In contrast to pluripotency genes, the cell lineage gene loci (e.g. *CDX2*, *GATA2*, *GATA4*, *SOX7* and *PDX1*) had high H3K27me3 and low H3K4me3 marks, respectively (Fig. 3i and Extended Data Fig. 8g).

Human EPSCs and porcine EPSCs shared similar signalling requirements revealed by removing individual components from the culture medium. Removal of the SRC inhibitor WH-4-023 or A-419259 reduced expression of pluripotency factors in both EPSCs (Extended Data Fig. 9a-d). Similar to mEPSCs [1], XAV939 enhanced AXIN1 protein content (Extended Data Fig. 9e), and reduced canonical WNT activities in both EPSCs (Extended Data Fig. 9f). Withdrawal of XAV939 caused collapse and differentiation of these EPSCs (Extended Data Fig. 9a-b, 9d, and 9g-k). SMAD2/3 were phosphorylated in EPSCs (Extended Data Fig. 9e). Either removing ACTIVIN A from pEPSCM or adding the TGFβ inhibitor SB431542 resulted in massive cell loss and down-regulation of pluripotency factors in pEPSCs (Extended Data Fig. 9a, 9g, 9h and 9j), whereas in human EPSCs, the TGFβ inhibitor SB431542 induced rapid cell differentiation with preferential expression of trophoblast lineage transcription factor genes *CDX2*, *ELF5* and *GATA2* (Extended Data Fig. 9b, 9i and 9k). At a relatively low concentration of exogenous ACTIVIN A (5.0ng/ml), hEPSCs showed a stronger propensity for embryonic mesendoderm lineage differentiation as demonstrated by higher lineage marker expression and production of NANOS3-tdTomato$^{+}$ cells [25] (Extended Data Fig. 9l-n). Removing CHIR99021 and Vitamin C from pEPSCM did not affect pluripotency gene expression but reduced the number of colonies from single cells (Extended Data Fig. 9a and 9h), whereas a high CHIR99021 concentration (3.0μM, H-CHIR99021) induced pEPSC$^{Emb}$ cell

differentiation (Extended Data Fig. 9a, 9h and 9j), similar to that in rat or human naïve cells [23, 35]. JNK and BRAF inhibition may improve the culture efficiency, but was not essential (Extended Data Fig. 9h-i). In hEPSCs, the requirements for CHIR99021 and Vc were similar to pEPSCs (Extended Data Fig. 9a-b and 9h-i).

The differentiation of hEPSCs to trophoblasts was tracked by expression of *CDX2-Venus* reporter (*T2A-Venus* inserted into the 3' UTR of the *CDX2* locusExtended Data Fig. 10a). Inhibiting TGFβ by SB431542 resulted in ~70% of the CDX2 reporter cells being CDX2-Venus$^+$ (Fig. 4a), whereas essentially no *CDX2-Venus*$^+$ cells were detected if the reporter cells were cultured in FGF or under the 5i naïve ESC conditions. Expression of trophoblast genes such as *CDX2*, *GATA3*, *ELF5*, *KRT7*, *TFAP2C*, *PGF*, *HAND1* and *CGA* rapidly increased in differentiating H1-EPSCs and iPSC-EPSCs but not H1-ESCs or H1-5i naïve cells (Fig. 4b). Addition of BMP4, which promotes differentiation of human ESCs to putative trophoblasts [36], induced expression of trophoblast genes at a much higher level in H1-EPSCs and iPSC-EPSCs than in H1-ESCs or H1-5i naïve ESCs (Extended Data Fig. 10b). Inhibiting FGF and TGFβ signalling while in parallel activating BMP4 effectively induced trophoblast differentiation in FGF-cultured human ESCs [37, 38]. Under this condition, expression of trophoblast genes, especially the late trophoblast genes *GCM1*, *CGA* and *CGB*, was much higher in H1-EPSCs than in H1-ESCs, whereas naïve 5i hESCs displayed no trophoblast differentiation (Extended Data Fig. 10c). Global gene expression analysis demonstrated that under TGFβ signalling inhibition H1-EPSCs and iPSC-EPSCs followed a distinct trajectory from the H1-ESCs (Fig. 4c), and that in cells differentiated from EPSCs, but not from H1-ESCs, important trophoblast development or function genes were highly expressed including *BMP4* (day 2-4

differentiation), genes of human endogenous retrovirus-encoded envelope protein *Syncytin-1* (*ERVW-1*) and *Syncytin-2* (*ERVFRD-1*) that promote cytotrophoblast fusion into syncytiotrophoblast, the maternally expressed gene *p57* (encoded by CDKN1C) which is expressed in trophoblast cells and is essential for normal placenta development [39, 40], *CD274* (encoding PD-L1 or B7-H1) that modulate immune cell activities, and *EGFR* which is important in human trophoblast stem cells (hTSCs) [41] (Extended Data Fig. 10d and Supplementary Table 6).

To further infer the identity of the differentiated hEPSCs by TGFβ inhibition, we performed Pearson correlation coefficient analysis of cells differentiated from H1-EPSCs, iPSC-EPSCs or H1-ESCs with external reference samples including primary human trophoblasts (PHTs) and the human placenta tissues [38], which again revealed the similarity between cells differentiated from hEPSCs and PHTs and the placenta (Extended Data Fig. 10e). The cells differentiated from H1-EPSCs by TGFβ inhibition expressed human trophoblast specific miRNAs (C19MC miRNAs: hsa-miR-525-3p, hsa-miR-526b-3p, hsa-miR-517-5p, and hsa-miR-517b-3p) [42] (Extended Data Fig. 10f-g), displayed DNA demethylation at the *ELF5* locus [43, 44] (Extended Data Fig. 10h), and produced abundant amounts of placental hormones (Extended Data Fig. 10i-j).

When hEPSCs (ESC-converted-EPSCs and iPSC-EPSCs) were cultured in human trophoblast stem cell (hTSC) conditions [41] under low cell density (2,000 cells/3.5cm dish), colonies with TSC morphology formed after 7-9 days (Fig. 4d). These colonies were picked and expanded into stable cell lines under hTSC condition with up to 30% line establishment efficiency (Fig. 4d). On the other hand, no hTSC lines could be established from standard human ESCs or human naïve ESCs (H1 and

M1 ESC). The hEPSC-derived TSCs expressed trophoblast transcription regulators: GATA2, GATA3 and TFAP2C, down-regulated pluripotency markers and could differentiate to both multi-nucleated syncytiotrophoblasts (ST) and HLA-G$^{+}$ extravillous trophoblasts (EVT) following the published protocols [41] (Fig. 4e, 4f and 4g and Extended Data Fig.11a-e). Although both pig and human EPSCs did not express placenta development-related genes such as *PGF*, *TFAP2C*, *EGFR*, *SDC1* and *ITGA5*, at high levels (Extended Data Fig. 8c), both cells had high H3K4me3 at these loci (Extended Data Fig. 11f), underpinning EPSCs' enhanced trophoblast potency. In line with the similarities between human and pig EPSCs, under human TSC condition, stable TSC-like lines could also be derived from pig EPSCs$^{Emb}$ (Extended Data Fig. 11g-i). Our results therefore provide compellingly evidence that human and pig EPSCs possessed expanded differentiation potential that encompasses the trophoblast lineage.

One of the key mechanisms for the derivation and maintenance of EPSCs of mouse, pig and human is blocking poly(ADP-ribosyl)ation activities of PARP family members TNKS1/2 using small molecule inhibitors such as XAV939 [45, 46]. In human cells, poly(ADP-ribose) is removed by poly(ADP-ribose) glycohydrolase (PARG) and ADP-ribosylhydrolase 3 (ARH3) [47]. Genetic inactivation of *Parp1/2* and *TNKS1/2* in the mouse caused trophoblast phenotypes, whereas inactivating *Parg* led to loss of functional trophectoderm and TSCs [48, 49]. We tested whether PARG was of any relevance to hEPSCs developmental potential to trophoblasts. In hEPSCs, *PARG*-deficiency did not appear to cause noticeable changes in EPSC culture but adversely affected trophoblast differentiation (Extended Data Fig. 12a-e), which may indicate an evolutionally conserved mechanism for EPSCs and trophoblast development from the mouse to human.

EPSCs of mouse, pig and human can now be established under similar *in vitro* culture conditions. These stem cells share unique molecular features and possess expanded potency for both embryonic and extraembryonic cell lineages that are generally not seen in the conventional embryo-derived or induced pluripotent stem cells. EPSCs may therefore represent a unique state of cellular potency. The successful generation of EPSCs produces new tools for investigation of embryonic development, and opens a wealth of avenues for translational research in biotechnology, agriculture, and genomics and regenerative medicine.

**References**


1. Yang, J., et al., *Establishment of mouse expanded potential stem cells.* Nature, 2017. **550**(7676): p. 393-397.
2. Ma, Y., et al., *Preserving self-renewal of porcine pluripotent stem cells in serum-free 3i culture condition and independent of LIF and b-FGF cytokines.* Cell Death Discov, 2018. **4**: p. 21.
3. Xue, B., et al., *Porcine Pluripotent Stem Cells Derived from IVF Embryos Contribute to Chimeric Development In Vivo.* PLoS One, 2016. **11**(3): p. e0151737.
4. Hou, D.R., et al., *Derivation of Porcine Embryonic Stem-Like Cells from In Vitro-Produced Blastocyst-Stage Embryos.* Sci Rep, 2016. **6**: p. 25838.
5. Park, J.K., et al., *Primed pluripotent cell lines derived from various embryonic origins and somatic cells in pig.* PLoS One, 2013. **8**(1): p. e52481.
6. Haraguchi, S., et al., *Establishment of self-renewing porcine embryonic stem cell-like cells by signal inhibition.* J Reprod Dev, 2012. **58**(6): p. 707-16.
7. Vassiliev, I., et al., *In vitro and in vivo characterization of putative porcine embryonic stem cells.* Cell Reprogram, 2010. **12**(2): p. 223-30.
8. Brevini, T.A., et al., *Culture conditions and signalling networks promoting the establishment of cell lines from parthenogenetic and biparental pig embryos.* Stem Cell Rev, 2010. **6**(3): p. 484-95.
9. Chen, L.R., et al., *Establishment of pluripotent cell lines from porcine preimplantation embryos.* Theriogenology, 1999. **52**(2): p. 195-212.
10. Esteban, M.A., et al., *Generation of induced pluripotent stem cell lines from Tibetan miniature pig.* J Biol Chem, 2009. **284**(26): p. 17634-40.
11. Ezashi, T., et al., *Derivation of induced pluripotent stem cells from pig somatic cells.* Proc Natl Acad Sci U S A, 2009. **106**(27): p. 10993-8.
12. Roberts, R.M., B.P. Telugu, and T. Ezashi, *Induced pluripotent stem cells from swine (Sus scrofa): why they may prove to be important.* Cell Cycle, 2009. **8**(19): p. 3078-81.
13. Wu, Z., et al., *Generation of pig induced pluripotent stem cells with a drug-inducible system.* J Mol Cell Biol, 2009. **1**(1): p. 46-54.

14. Telugu, B.P., T. Ezashi, and R.M. Roberts, *Porcine induced pluripotent stem cells analogous to naive and primed embryonic stem cells of the mouse.* Int J Dev Biol, 2010. **54**(11-12): p. 1703-11.
15. West, F.D., et al., *Porcine induced pluripotent stem cells produce chimeric offspring.* Stem Cells Dev, 2010. **19**(8): p. 1211-20.
16. Zhang, W., et al., *Pluripotent and Metabolic Features of Two Types of Porcine iPSCs Derived from Defined Mouse and Human ES Cell Culture Conditions.* PLoS One, 2015. **10**(4): p. e0124562.
17. Petkov, S., et al., *Long-Term Culture of Porcine Induced Pluripotent Stem-Like Cells Under Feeder-Free Conditions in the Presence of Histone Deacetylase Inhibitors.* Stem Cells Dev, 2016. **25**(5): p. 386-94.
18. Wang, H., et al., *Induction of Germ Cell-like Cells from Porcine Induced Pluripotent Stem Cells.* Sci Rep, 2016. **6**: p. 27256.
19. Lai, S., et al., *Generation of Knock-In Pigs Carrying Oct4-tdTomato Reporter through CRISPR/Cas9-Mediated Genome Engineering.* PLoS One, 2016. **11**(1): p. e0146562.
20. Du, X., et al., *Barriers for Deriving Transgene-Free Pig iPS Cells with Episomal Vectors.* Stem Cells, 2015. **33**(11): p. 3228-38.
21. Theunissen, T.W., et al., *Systematic identification of culture conditions for induction and maintenance of naive human pluripotency.* Cell stem cell, 2014. **15**(4): p. 471-87.
22. Ying, Q.L., et al., *The ground state of embryonic stem cell self-renewal.* Nature, 2008. **453**(7194): p. 519-23.
23. Takashima, Y., et al., *Resetting Transcription Factor Control Circuitry toward Ground-State Pluripotency in Human.* Cell, 2014. **158**(6): p. 1254-69.
24. Hayashi, K., et al., *Reconstitution of the mouse germ cell specification pathway in culture by pluripotent stem cells.* Cell, 2011. **146**(4): p. 519-32.
25. Kobayashi, T., et al., *Principles of early human development and germ cell program from conserved model systems.* Nature, 2017. **546**(7658): p. 416-420.
26. Irie, N., et al., *SOX17 is a critical specifier of human primordial germ cell fate.* Cell, 2015. **160**(1-2): p. 253-68.
27. Gkountela, S., et al., *The ontogeny of cKIT+ human primordial germ cells proves to be a resource for human germ line reprogramming, imprint erasure and in vitro differentiation.* Nat Cell Biol, 2013. **15**(1): p. 113-22.
28. Julaton, V.T. and R.A. Reijo Pera, *NANOS3 function in human germ cell development.* Hum Mol Genet, 2011. **20**(11): p. 2238-50.
29. International Stem Cell, I., et al., *Characterization of human embryonic stem cell lines by the International Stem Cell Initiative.* Nat Biotechnol, 2007. **25**(7): p. 803-16.
30. Koyanagi-Aoi, M., et al., *Differentiation-defective phenotypes revealed by large-scale analyses of human pluripotent stem cells.* Proc Natl Acad Sci U S A, 2013. **110**(51): p. 20569-74.
31. Wang, W., et al., *Rapid and efficient reprogramming of somatic cells to induced pluripotent stem cells by retinoic acid receptor gamma and liver receptor homolog 1.* Proc Natl Acad Sci U S A, 2011. **108**(45): p. 18283-8.
32. Yan, L., et al., *Single-cell RNA-Seq profiling of human preimplantation embryos and embryonic stem cells.* Nat Struct Mol Biol, 2013. **20**(9): p. 1131-9.
33. Dang, Y., et al., *Tracing the expression of circular RNAs in human pre-implantation embryos.* Genome Biol, 2016. **17**(1): p. 130.
34. Blakeley, P., et al., *Defining the three cell lineages of the human blastocyst by single-cell RNA-seq.* Development, 2015. **142**(20): p. 3613.
35. Chen, Y., K. Blair, and A. Smith, *Robust Self-Renewal of Rat Embryonic Stem Cells Requires Fine-Tuning of Glycogen Synthase Kinase-3 Inhibition.* Stem cell reports, 2013. **1**(3): p. 209-17.

36. Xu, R.H., et al., *BMP4 initiates human embryonic stem cell differentiation to trophoblast.* Nat Biotechnol, 2002. **20**(12): p. 1261-4.
37. Amita, M., et al., *Complete and unidirectional conversion of human embryonic stem cells to trophoblast by BMP4.* Proc Natl Acad Sci U S A, 2013. **110**(13): p. E1212-21.
38. Yabe, S., et al., *Comparison of syncytiotrophoblast generated from human embryonic stem cells and from term placentas.* Proc Natl Acad Sci U S A, 2016. **113**(19): p. E2598-607.
39. Chilosi, M., et al., *Differential expression of p57kip2, a maternally imprinted cdk inhibitor, in normal human placenta and gestational trophoblastic disease.* Lab Invest, 1998. **78**(3): p. 269-76.
40. Zhang, P., et al., *Cooperation between the Cdk inhibitors p27(KIP1) and p57(KIP2) in the control of tissue growth and development.* Genes Dev, 1998. **12**(20): p. 3162-7.
41. Okae, H., et al., *Derivation of Human Trophoblast Stem Cells.* Cell Stem Cell, 2018. **22**(1): p. 50-63 e6.
42. Lee, C.Q., et al., *What Is Trophoblast? A Combination of Criteria Define Human First-Trimester Trophoblast.* Stem Cell Reports, 2016. **6**(2): p. 257-72.
43. Hemberger, M., et al., *ELF5-enforced transcriptional networks define an epigenetically regulated trophoblast stem cell compartment in the human placenta.* Hum Mol Genet, 2010. **19**(12): p. 2456-67.
44. Ng, R.K., et al., *Epigenetic restriction of embryonic cell lineage fate by methylation of Elf5.* Nat Cell Biol, 2008. **10**(11): p. 1280-90.
45. Huang, S.M., et al., *Tankyrase inhibition stabilizes axin and antagonizes Wnt signalling.* Nature, 2009. **461**(7264): p. 614-20.
46. Thorsell, A.G., et al., *Structural Basis for Potency and Promiscuity in Poly(ADP-ribose) Polymerase (PARP) and Tankyrase Inhibitors.* J Med Chem, 2017. **60**(4): p. 1262-1271.
47. Hassa, P.O. and M.O. Hottiger, *The diverse biological roles of mammalian PARPS, a small but powerful family of poly-ADP-ribose polymerases.* Front Biosci, 2008. **13**: p. 3046-82.
48. Koh, D.W., et al., *Failure to degrade poly(ADP-ribose) causes increased sensitivity to cytotoxicity and early embryonic lethality.* Proc Natl Acad Sci U S A, 2004. **101**(51): p. 17699-704.
49. Hemberger, M., et al., *Parp1-deficiency induces differentiation of ES cells into trophoblast derivatives.* Developmental biology, 2003. **257**(2): p. 371-81.

## Acknowledgements

We thank colleagues of the Wellcome Trust Sanger Institute core facilities for generous supports (James Bussell, Yvette Hooks, N. Smerdon, B. L. Ng and J. Graham), Professor Ashley Moffett for critical comments. We acknowledge the following funding and supports: The Wellcome Trust (grant numbers 098051 and 206194) to the Sanger Institute, and The University of Hong Kong internal funding (P. Liu); Wellcome Trust Clinical PhD Fellowship for Academic Clinicians (D.J.R.);

PhD fellowship (Portuguese Foundation for Science and Technology, FCT (SFRH/BD/84964/2012) (L.A.), Marie Sklodowska-Curie Individual Fellowship (M.A.E.-M.); BBSRC (grant BB/K010867/1), Wellcome Trust (grant 095645/Z/11/Z), EU EpiGeneSys, and BLUEPRINT to (W.R.); Chongqing Agriculture Development Grant (17407 for L.P.G., Z.H.L., and Y.H.; REBIRTH project No. 9.1, Hannover Medical School (MHH) (for H.N.); National Natural Science Foundation (81671579), Shuguang Planning of Shanghai Municipal Education Commission (16SG14) and The National Key Research and Development Program (2017YFA0104500) (LLu); China Postdoctoral Science Foundation (grant 2017M622795) (DC); Shenzhen Municipal Government of China (DRC-SZ [2016] 884) (ZS) NHMRC of Australia (PPLT, Senior Principal Research Fellowship, Grant 1110751 (PPLT). The current address of Dr. Stoyan Petkov: German Primate Center, Platform Degenerative Diseases Kellnerweg 4, 37077 Goettingen, Germany.

**Author contributions**

X.G. developed the culture conditions for pEPSCs and hEPSCs and performed most of the experiments; MN performed the pig experiments and wrote the paper; SP provided some pig reprogramming factor genes; XC performed most of the informatics analysis and ST supported XC; DC, SW and ZS analyzed RNAseq data of hEPSCs/ESCs to trophoblasts; MEM and WR performed EPSC global DNA methylation analysis; TK and AS supported XG on PGCLC analysis; AH and AA measured hormones in cells differentiated from hEPSCs; LC analysed teratoma sections; YF and FB karyotyped cells; DR, XW, LG, ZL, YH, TN, DW, DP, LLai, GL, DRyan, JY, LA, YY, SGX, YZ, LLu, ZX were involved in refining the culture conditions or intellectual inputs; SJK provided human M1 and M10 cells; PPLT

provided intellectual inputs and edited the manuscript; HN conceptualized pig experiments, wrote paper, secured funding for the pig part of the experiments; PL conceived the pEPSC culture condition screen concept, supervised the research and wrote paper.

## Figure legends

**Figure 1**. Derivation and characterization of pig EPSCs. **a**. Left: Schematic diagram of establishment of pig EPSC$^{Emb}$ lines from German Landrace day-5 *in vivo* derived blastocysts on STO feeder cells in pEPSCM, and of pEPSC$^{iPS}$ lines by reprogramming German Landrace PFFs and China TAIHU *OCT4-Tdtomato* knock-in reporter (POT) PFFs. Right panels: images of established EPSC lines, and fluorescence image of Td-tomato expression in POT-pEPSC$^{iPS}$. Three EPSC$^{Emb}$ lines (Male: K3 and K5; Female K1) and three pEPSC$^{iPS}$ lines (#10, #11) were extensively tested in this study. These EPSC lines behaved similarly in gene expression and differentiation. **b**. Bisulphite sequencing analysis of CpG sites in the *OCT4* and *NANOG* promoter regions in PFFs, pEPSC$^{iPS}$ and pEPSC$^{Emb}$. **c**. Gene expression in embryoid bodies (EBs, day 7) of pEPSCs$^{Emb}$. Genes of both embryonic and extra-embryonic cell lineages were examined in RT-qPCR. Data are mean ± s.d. (n = 3). **d**. Tissue composition of pEPSC$^{Emb}$ teratoma sections (H&E staining): Examples of glandular epithelium derived from endoderm (i), cartilage derived from mesoderm (ii), immature neural tissue derived from ectoderm, which forms well defined neural tubes (iii), and large multinucleated cells reminiscent of torphoblasts (arrows in iv). **e**. Expression of PL-1 in multi-nucleated cells in the pEPSC$^{Emb}$ teratoma sections revealed by immunostaining. **f**. Schematic diagram of day 25-27 pig chimera embryos. The circles mark the areas where tissues taken for immunofluorescence analysis (Additional chimeras tissues were analysed in Extended Data Fig. 5e, 5f): i, brain; ii, liver. **g**. Detection of pEPSC descendants in the brain (H2BmCherry$^{+}$SOX2$^{+}$) and the liver (H2BmCherry$^{+}$AFP$^{+}$) cells in chimera $^{\#}$16. Nuclei were stained with DAPI. Boxed areas are shown in higher magnification.

**Figure 2**. *In vitro* generation of PGC-like cells from pEPSCs$^{Emb}$. **a**. Induction of pPGCLC by transiently expressing *SOX17* in *NANOS3-H2BmCherry* reporter pEPSCs. The presence of H2BmCherry$^{+}$TNAP$^{+}$ cells in embryoid bodies (EBs) were analysed by FACS. **b**. RT-qPCR analysis of PGC genes in day 3 EBs following pPGCLC induction. **c**. Immunofluorescence analysis PGC factors in the sections of day 3-4 EBs of pPGCLC induction. The H2BmCherry$^{+}$ cells co-expressed NANOG, OCT4, BLIMP1, TFAP2C and SOX17. Nuclei were stained with DAPI. Experiments were repeated at least three times. **d**. RNAseq analysis (Heat map) of sorted H2BmCherry$^{+}$ of pPGCLC induction shows expression of genes associated with PGCs, pluripotency or somatic lineages (mesoderm, endoderm, and gonadal somatic cells). **e**. Pair-wise gene expression comparison between pEPSCs$^{Emb}$ and pPGCLCs. Key up-regulated (red) and down-regulated (blue) genes were highlighted. **f**. Bar plot shows expression of genes related to DNA methylation in pPGCLCs and the parental pEPSCs$^{Emb}$. Data are from RNAseq of sorted H2BmCherry$^{+}$ of pPGCLC induction.

**Figure 3**. Establishment of human EPSCs. **a**. Images of the established H1-EPSCs or M1-EPSCs (passage 25). **b**. Principal component analysis (PCA) of bulk RNA-seq gene expression data of human, pig and mouse EPSCs, human primed and naïve ESCs, PFFs. pEPSC$^{Par}$: EPSC lines from parthenogenetic embryos; E14 and AB2-EPSCs are mouse EPSCs. **c**. Pair-wise comparison of gene expression between H1-ESCs and H1-EPSCs, showing the highly expressed genes (>8 folds) in hEPSCs (total 76, red dots) and representative histone genes (blue dots). **d**. Heatmap showing expression of selected histone genes in H1-ESCs, H1-EPSCs, iPSC-EPSCs and human naïve (5i) ESCs, and human preimplantation embryos. The RNAseq data of human primed and naïve ESCs were obtained from Theunissen, T. W. et al. (Cell Stem Cell 2014) whereas embryo cell data were from Yan L., et al (Nat Struct Mol

Biol. 2013). **e**. RT-qPCR analysis of expression of four histone 1 cluster genes in seven human ESC or iPSC lines cultured in the three conditions: FGF (primed), 5i (naïve) and EPSCM (EPSC). Hipsci iPSC lines were obtained from the Hipsc project at the Wellcome Trust Sanger Institute (http://www.hipsci.org): #1, HPSI1113i-bima_1; #2, HPSI1113i-qolg_3; #3, HPSI1113i-oaaz_2; #4, HPSI1113i-uofv_1. Relative expression levels, normalized to *GAPDH*, are compared against that in the cells cultured in the FGF condition. Data are mean ± s.d. (n = 3). Experiments were repeated at least three times. **f**. Violin plots show scRNAseq expression of pluripotency genes in pEPSCs$^{Emb}$ (top panel) and human H1-EPSCs (lower panel). **g**. PCA of global gene expression pattern (by scRNAseq) of pEPSCs$^{Emb}$ (left panel) and H1-EPSCs (right panel). **h**. PCA and comparison of gene expression from scRNAseq of human H1-EPSCs and human preimplantation embryos (Yan L. 2013 Nat Struct Mol Biol. See Methods for details) . **i**. ChIP-seq analysis of H3K27me3 and H3K4me3 marks at pluripotency gene loci in pEPSCs$^{Emb}$ and human H1-EPSCs.

**Figure 4**. Trophoblast differentiation potential of human EPSCs. **a**. Left panel: diagram of hEPSCs to trophoblast under TGFβ inhibition. See Methods for more details. Right panel: differentiation the *CDX2-H2B-Venus* reporter EPSCs to trophoblasts detected in flow cytometry. The *CDX2-H2B-Venus* reporter EPSCs were also cultured in conventional FGF-containing hESCs medium or 5i-naïve medium and were subsequently subjected to the same differentiation condition and examined in flow cytometry. Cells were collected 4 days after TGFβ inhibition. **b**. The dynamic changes in the expression of trophoblast genes during hEPSC differentiation at several time points assayed by RT-qPCR. Data are mean ± s.d. (n = 3). Experiments were repeated at least three times. **c**. tSNE analysis of RNA-seq data of the differentiated cells from H1-ESCs, H1-EPSCs, or iPSC-EPSCs treated with the TGFβ

inhibitor SB431542. RNAs were sampled at Day 0-12 during differentiation. The differentiation trajectory of H1-EPSCs and hiPSC-EPSCs is distinct from that of H1-ESCs. **d**. Phase-contrast images of primary TSC colonies formed from individual hEPSCs (left) and of TSCs at passage 7 (right). **e**. Expression of trophoblast transcription factors GATA3 and TFAP2C, and KRT7 in EPSC-TSCs detected by immunostaining. Nuclei were stained with DAPI. Similar results were obtained with four independent EPSC-TSC lines. **f**. Expression of SDC1 in syncytiotrophoblasts differentiated from EPSC-TSCs detected by immunofluorescence. DAPI stains the nucleus. **g**. Detection of HLA-G in hESCs, hEPSCs, hTSCs, and the cells differentiated from hTSCs following the EVT protocol (Okae, H, et al. Cell Stem cell 2018). The choriocarcinoma cells JEG-3 that are representatives of extravillous trophoblasts and express HLA-G, and JAR that are representatives of villous trophoblast cells so do not express any HLA molecules (Apps, R., et al. Immunology 2009), were used as the positive and negative control, respectively. Experiments were repeated at least three times.

## Extended Data Figures

**Extended Data Figure 1**. Establishment of new Dox-dependent pig iPSC lines for screening culture conditions. **a**. Doxycycline (Dox)-inducible expression of Yamanaka factors *OCT4*, *MYC, SOX2* and *KLF4*, together with *LIN28*, *NANOG*, *LRH1* and *RARG* in wild type German Landrace PFFs. cDNAs were cloned into *piggyBac* (PB) vectors and transfected into PFFs with a plasmid expressing the PB transposase for stable integration of the expression cassette into the pig genome. OMSK: 4 Yamanaka factors *OCT4*, *MYC, SOX2* and *KLF4;* N-LIN: NANOG and LIN28; RL: RARG and LRH1. After 8-10 days of Dox induction, primary colonies appeared. Those colonies were single-cell passaged in the presence of Dox in M15 (15% fetal calf serum). **b**. Co-expression of *LIN28*, *NANOG*, *LRH1* and *RARG* substantially increased the number of reprogrammed colonies. *p value < 0.05: the 8-factor induced colonies from 250,000 PFFs in comparison to those of using 4 Yamanaka factors. **c**. Reprogramming of the porcine *OCT4-tdTomato* knock-in reporter (POT) TAIHU PFFs to iPSCs. After 8 days of Dox induction, the primary colonies appeared, which were $tdTomato^{+}$ under fluorescence microscope. The primary colonies were picked and expanded in the presence of Dox. Shown on image are P3 cells of bright field and fluorescence. **d**. The iPSCs lines expressed key pluripotency genes in RT-qPCR analysis. The iPSC lines $^{\#}1$ and $^{\#}2$, and iPSC $^{\#}3$ and $^{\#}4$ were from wild type German Landrace and TAIHU POT PFFs, respectively. Gene expression in pig parthenogenetic blastocysts was used as the control. **e**. RT-qPCR analysis of expression of the exogenous reprogramming factors in iPSCs either in the presence of Dox or 3 days after its removal. **f**. Differentiation of iPSC cells once Dox was removed from the culture medium. The images were cells 3 days after Dox removal. The POT iPSCs became Td-tomato negative. **g**. RT-qPCR analysis of the

674 expression of endogenous pluripotency genes in iPSC cultured with or without Dox.
675 **h**. Expression of lineage genes in the pig iPSCs 5-6 days after DOX removal. Gene
676 expression was measured by RT-qPCR. Data are mean ± s.d. (n = 3). Experiments
677 were repeated at least three times.

678 **Extended Data Figure 2**. Identification of culture conditions for pig EPSCs. **a**. The
679 Dox-dependent iPSC clone $^{\#}$1 of German Landrace strain was used in the screens.
680 Small molecule inhibitors and cytokines were selected for various combinations. Cell
681 survival, cell morphology, and expression of endogenous *OCT4* and *NANOG* were
682 employed as the read-outs. **b-h**. The relative expression levels of endogenous *OCT4*
683 and *NANOG* in the survived cells after 6 days of culture in different basal media
684 supplemented with inhibitors and cytokines combinations: **b**. M15 medium without
685 Dox; **c**. N2B27 basal medium without Dox; **d**. 20% KOSR medium without Dox; **e**.
686 AlbumMax II basal medium without Dox; **f**. N2B27 basal medium with Dox; **g**. Four
687 individual basal medium with Dox (M15: 411-431; N2B27: 432-453; KOSR: 454-
688 475; AlbumMax II: 476-497); **h**. N2B27 basal medium without Dox. 2i: GSK3i and
689 MEKi; t2i: GSK3i, MEKi and PKCi (Takashima, Y., et al. 2014 Cell); 4i: GSK3i,
690 MEKi, JNKi and p38i (Irie, N., et al 2015 Cell); 5i: GSK3i, MEKi, ROCKi, BRAFi
691 and SRCi (Theunissen, T. W., et al. 2014 Cell Stem Cell); mEPSCM: GSK3i, MEKi,
692 JNKi, XAV939, SRCi and p38i ( Yang J ., et al. 2017 Nature); Details of the inhibitor
693 combinations are presented in Supplementary Table 1. The experiments in Extended
694 Data Figure 2h were repeated at least three times.

695 **Extended Data Figure 3**. Establishment of pig EPSCs by reprogramming PFFs or
696 from pre-implantation embryos. **a**. Images showing the toxicity of MEKi, PKCi and
697 p38i to the pig iPSCs in M15 plus Dox. **b**. Endogenous pluripotency gene expression
698 in both wild type and *OCT4-TdTomato* reporter iPSCs in the absence of Dox in

699 pEPSCM (#517 minimal condition, Extended Data Fig. 2h). Gene expression was
700 compared to that in porcine parthenogenetic blastocysts. Data are mean ± s.d. (n = 3).
701 **c**. Images of wild type and *OCT4-Tdtomato* reporter iPSCs in pEPSCM without Dox.
702 Gene expression was compared to that in porcine parthenogenetic blastocysts. **d**.
703 Detection of leaky expression of the exogenous reprogramming factors by RT-PCR.
704 About half of the iPSC lines did not have detectable leaky expression. **e**. Schematic
705 diagram of reprogramming PFFs to establish EPSC lines in pEPSCM. **f**. Two newly
706 established WT pEPSC$^{iPS}$ lines (#10 and #11) were examined for the expression of
707 endogenous pluripotency genes and the exogenous reprogramming factors. Data are
708 mean ± s.d. (n = 3). **g**. Day-10 outgrowth from a porcine early blastocyst in pEPSCM
709 supplemented with ROCK inhibitor. The outgrowths were picked at day 10-12 for
710 dissociation and re-plating to establish stable lines. **h**. Representative images of the
711 pEPSC$^{Emb}$ (Line K3) established from pig *in vivo* derived embryos. Experiments were
712 repeated at least three times.

713 **Extended Data Figure 4**. Characterisation of pEPSCs. **a**. pEPSC$^{Emb}$ (Line K3)
714 retained the normal karyotype after 25 passages (10/10 metaphase spreads examined
715 were normal). Two additional lines examined also had the normal karyotype after
716 more than 25 passages. **b**. Immunostaining detection of pluripotency factors and
717 markers, SSEA-1 and SSEA-4, in pEPSC$^{Emb}$ and pEPSC$^{iPS}$. **c**. Active *Oct4* distal
718 enhancer in pig EPSC$^{Emb}$ and EPSC$^{iPS}$. The mouse *Oct4* distal and proximal enhancer
719 constructs were used in the luciferase assay. Data are mean ± s.d. (n = 3). **d**. Efficient
720 genome-editing in pEPSCs$^{Emb}$. Knocking-in the H2B-mCherry expressing cassette
721 into pig *ROSA26* locus was facilitated by the CRISPR/Cas9. Out of 20 colonies
722 picked for genotyping, 5 were correctly targeted. Importantly, the targeted pEPSCs
723 retained the normal karyotype. **e**. Bright field and fluorescence images of the

724 pEPSC$^{Emb}$ colonies with the *H2B-mCherry* correctly targeted to the *ROSA26* locus. **f.**
725 *in vitro* differentiation of pEPSC$^{Emb}$ to cells of the three somatic germ layers and the
726 trophectoderm lineage (KRT7$^{+}$).

727 **Extended Data Figure 5**. *In vivo* differentiation potential of pEPSCs. **a**. Participation
728 of pEPSCs in preimplantation embryo development. H2B-mCherry-expressing donor
729 pEPSCs$^{iPS}$ were injected to day 5 host pig parthenogenetic embryos, which were
730 allowed to develop into blastocysts. Arrow indicates donor cell's location in the TE.
731 H2BmCherry$^{+}$ donor cells were found in both the inner cell mass and the
732 trophectoderm. **b**. Whole-mount fluorescence and bright field images of 26-day pig
733 embryos from the preimplantation embryos injected with H2BmCherry$^{+}$ pEPSCs$^{Emb}$,
734 showing the possible presence of mCherry$^{+}$ cells in chimera #21. **c**. Tissues were
735 dissected out from four areas of each embryo, head (a), trunk (b) and tail (c), and the
736 placenta (d), which were dissociated to single cells for flow cytometry analysis to
737 detect donor H2BmCherry$^{+}$ cells and for making genomic DNA samples for PCR
738 analysis. **d**. PCR genotyping for mCherry DNA using the genomic DNA samples
739 described above. mCherry DNA was only detected in the embryos that were
740 mCherry$^{+}$ by flow cytometry analysis. **e.** Schematic diagram of day 25-27 pig chimera
741 embryos. The circles mark the tissue areas that were taken for immunostaining
742 analysis as shown in the main Fig. 1f. iii: neural tissues; iv: endoderm derivatives; v:
743 smooth muscle; vi: the placenta. **f**. Co-localisation of H2BmCherry with lineage
744 markers in the mCherry$^{+}$ fetuses and placentas using antibodies to TUJ1 (Chimera
745 #16), SOX17 (Chimera #21), GATA4 (Chimeras #21), a-SMA (Chimera #21), KRT7
746 and PL-1 (Chimera #6) on cryosections by immunofluorescence.

747 **Extended Data Figure 6**. Differentiation of pEPSCs to pPGCLCs. **a**. Generation of
748 the *NANOS3-H2BmCherry* reporter EPSCs$^{Emb}$ by targeting the *H2B-mCherry* cassette

749 to the *NANOS3* locus. In the targeted allele, the *T2A-H2B-mCherry* sequence was in
750 frame with the last coding exon of the pig *NANOS3* locus with the stop codon TAA
751 being deleted. We generated gRNA plasmids targeting specifically to the region
752 covering the *NANOS3* stop codon. We picked 15 colonies for genotyping, and 4 of
753 them were correctly targeted ones. After expansion, those targeted pEPSCs were
754 found retaining the normal karyotype. **b**. Diagram illustrating the strategy for
755 expressing exogenous genes in pEPSCs$^{Emb}$ for pPGCLC specification and
756 differentiation (see Methods for more details). **c**. Expressing *NANOG*, *BLIMP1* and
757 *TFAP2C* individually or in combination with *SOX17* in the differentiation of
758 *NANOS3-H2BmCherry* reporter EPSCs$^{Emb}$ to pPGCLCs (H2BmCherry$^{+}$). **d**. RT-
759 qPCR analysis of PGC genes. RNA samples were prepared from day 3 EBs of
760 pEPSCs that expressed transgenes individually or in combinations following the
761 pPGCLC induction protocol in **b**. Relative expression levels are shown with
762 normalization to *GAPDH*. Data are mean ± s.d. (n = 3). Experiments were repeated at
763 least three times.

764 **Extended Data Figure 7**. Establishment and characterisation of human EPSCs. **a**.
765 Images of H1, H9, M1 and M10 human ESC colonies in pEPSCM or in pEPSCM
766 minus Activin A. Expression of OCT4 was detected by immunostaining. **b**. Normal
767 karyotype in H1-EPSCs and M1-EPSCs after 25 passages in hEPSCM (10/10
768 metaphases scored were normal). **c**. Primary iPSC colony (top) and established
769 cultures of iPSCs (bottom) in hEPSCM reprogrammed from human dermal fibroblasts
770 by Dox-inducible expression of exogenous *OCT4*, *MYC*, *KLF4*, *SOX2*, *LRH1* and
771 *RARG*. **d**. The relative expression levels of pluripotency genes (*POU5F1*, *SOX2*,
772 *NANOG*, *REX1* and SALL4) in H1-ESCs, H1-naïve ESCs (5i), H1-EPSCs and iPSC-
773 EPSCs. *p value < 0.05 compared with H1-naïve ESCs (5i), H1-EPSCs and iPSC-

EPSCs. Data are mean ± s.d. (n = 3). **e**. Detection of potential expression leakiness of the exogenous reprogramming factors by RT-qPCR. No obvious leakiness was found in the four established iPSC lines. **f**. The relative doubling time of H1-ESCs, H1-naïve ESCs (5i), H1-EPSCs and iPSC-EPSCs. Data are mean ± s.d. (n = 3). *p value < 0.05. **g**. Expression of lineage markers (*EOMES*, *GATA4*, *GATA6*, *T*, *SOX17* and *RUNX1*) in H1-ESCs, H1-naïve ESCs (5i), H1-EPSCs and iPSC-EPSCs. Data are mean ± s.d. (n = 3). **h**. Immunostaining of H1-EPSCs and iPSC-EPSCs for pluripotency factors and cell surface markers. **i.** *In vitro* differentiation of H1-EPSCs to the three somatic cell lineages. **j.** Teratomas from hEPSCs in immunocompromised mice showing by morphology the presence of cartilage (mesoderm. I), glandular epithelium (endoderm. II) and mature neural tissue (glia and neurons, ectoderm. III) in H&E staining. **k**. EBs of H1-EPSCs to PGCLCs immunostained for OCT4, BLIMP1 and SOX17. **l**. FACS analysis for expression of CD38 and TNAP on PGCLCs of H1-EPSCs. The induction of PGCLCs was performed on at least two independent human EPSC lines, and experiments were repeated at least three times.

**Extended Data Figure 8**. Molecular features of human and porcine EPSCs. **a**. Hierarchical clustering of global gene expression data (RNA-seq) of human primed and naïve ESCs, EPSCs of human, pig and mouse. Correlation matrix was clustered using Spearman correlation and complete linkage. pEPSC$^{Par}$: EPSC lines from porcine parthenogenetic embryos; E14 and AB2-EPSCs are mouse EPSCs. See Methods for details of data resources for this analysis. **b.** Expression of pluripotency and lineage genes in pig (left panel) and human (right panel) EPSCs. **c.** Expression of trophoblast related genes in pig (left panel) and human (right panel) EPSCs. **d**. Global DNA methylation levels in pig (left) and human (right) EPSCs. **e**. Expression of genes encoding enzymes in DNA methylation or demethylation in pig (left) and human

(right) EPSCs. Data are mean ± s.d. (n = 3). **f**. PCA of scRNAseq data of human H1-EPSCs and that of human preimplantation embryos (data from Dang Y. et al 2016. Genome Biology. See Methods for more details). **g**. Histone modifications (H3K4me3 and H3K27me3) at the loci for genes encoding enzymes involved in DNA methylation and demethylation and for lineage genes.

**Extended Data Figure 9**. The requirement of individual components in the culture conditions for pig EPSCs and human EPSCs. **a-b**. The effects of removing individual inhibitors on gene expression in $pEPSCs^{Emb}$ and H1-EPSCs analysed by RT-qPCR. "-SRCi, -XAV939, -ACTIVIN, -Vc, -CHIR99": removing them individually from pEPSCM or hEPSCM; "+TGFBi, +H-CHIR99": adding the TGFβ inhibitor SB431542, or a higher concentration of CHIR99021 (3.0 μM). **c**. Targeting the *OCT4-H2B-Venus* cassette into the *OCT4* locus in H1-EPSCs. In the targeted allele, the *T2A-H2B-Venus* sequence was in frame with the last coding exon of the *OCT4* gene. The stop codon TGA was deleted. We genotyped 19 colonies, 5 of them were correctly targeted. **d**. The effects of removing the SRC inhibitor WH-4-023 or XAV939 from hEPSCM measured by $Venus^{+}$ cells. The *OCT4-H2B-Venus* reporter EPSCs were cultured in the indicated conditions and were analysed for Venus expression by fluorescence microscopy or in flow cytometry. **e**. Western blot analysis of AXIN1 and phosphorylation of SMAD2/3 in porcine and human EPSCs. Both $pEPSC^{Emb}$ and H1-EPSCs had much higher levels of AXIN1. $pEPSC^{Emb}$, H1-EPSCs and H1-naïve ESCs (5i) had higher levels of TGFβ signalling evidenced by higher pSMAD2/3 than in the differentiated (D) $EPSC^{Emb}$ or primed H1-ESCs. **f**. TOPflash analysis of the canonical Wnt signalling activities in porcine and human EPSCs. Removing XAV939 from pEPSCM (pEPSCM-X) or hEPSCM (hEPSCM-X) substantially increased TOPflash activity. *$p < 0.05$. RT-qPCR data are mean ± s.d. (n

= 3). Experiments were repeated at least three times. **g**. Bright-field and immunofluorescence images showing pEPSCs$^{Emb}$ cultured in pEPSCM or in pEPSCM with the indicated changes in its components. The cells were stained for OCT4. **h-i**. Quantitation of AP$^{+}$ colonies formed from 2,000 pEPSCs$^{Emb}$ or H1-EPSCs on STO feeders in a 6-well plate. The colonies were scored for 5 consecutive passages to determine the effects of removing XAV939, Vitamin C or CHIR99021, or of adding a JNK inhibitor or a BRAF inhibitor. Data are mean ± s.d. (n = 3) and the experiments were repeated three times. **j-k**. RT-qPCR analysis of expression of lineage genes in pEPSCs$^{Emb}$ and hEPSCs when XAV939 or ACTIVIN A was removed from pEPSCM and hEPSCM or TGFB signalling was inhibited by SB431542. **l**. The effects of supplementing 5.0 ng/ml ACTIVIN A in hEPSCM on the expression of lineage genes in EBs formed from H1-EPSCs. Genes of mesendoderm lineage genes were substantially increased. *p < 0.05. **m-n**. Differentiation to PGCLCs from the NANOS3-Tdtomato reporter EPSCs cultured in hEPSCM either with or without 5.0ng/ml ACTIVIN A. Adding ACTIVIN A substantially increased PCGLCs measured in FACS (Tdtomato$^{+}$). RT-qPCR analysis of PGCLC genes confirmed the increase of PCGLCs. *p < 0.05 in comparison to hEPSCM supplemented with ACTIVIN A. RT-qPCR data are mean ± s.d. (n = 3). Experiments were repeated at least three times.

**Extended Data Figure 10**. Characterization of hEPSC trophoblast differentiation potential. **a**. Generation of the *CDX2-H2BVenus* reporter EPSC line. In the targeted allele, the *T2A-H2BVenus* sequence was in frame with the last coding exon of the human *CDX2* gene. The TGA stop codon was deleted in the targeted allele. The reporter EPSCs were subsequently cultured in hEPSCM, in the standard FGF-containing human ESC medium or in the 5i condition for human naïve ESCs, for

subsequent analyses. **b**. Trophoblast gene expression measured by RT-qPCR in cells induced to differentiate to trophoblasts by 4-day BMP4 treatment. Experiments were repeated at least three times. **c**. Trophoblast gene expression measured by RT-qPCR in hEPSC induced to differentiate to trophoblasts by SB431542 + PD173074 + BMP4. qRT-PCR data are mean ± s.d. (n = 3). Cells were collected at several time points for analysis. **d**. Heatmap shows expression changes of trophoblast genes in cells differentiated from H1-ESCs (green), H1-EPSCs (red) or iPSC-EPSCs (blue) (RNAseq data are in Supplementary Table 6). Cells were collected at several differentiation time points for RNAseq analysis. **e**. Pearson correlation coefficient of gene expression in cells differentiated from H1-ESCs, H1-EPSCs and iPSC-EPSCs (RNAseq data in Supplementary Table 6), with the published data of PHTu and PHTd (undifferentiated and differentiated human primary trophoblasts, respectively) and with human tissues. The details of these analyses are in Methods. **f**. Detection of the four C19MC miRNAs (hsa-miR-525-3p, -526b-3p, -517-5p, and -517b-3p) in cells differentiated from H1-EPSCs, H1-ESCs, H1-naïve ESCs (5i) and iPSC-EPSCs treated with SB431542 for six days. The choriocarcinoma cells JEG-3 that are representatives of extravillous trophoblasts and JAR that are representatives of villous trophoblast cells were used as the positive and negative control, respectively. **g**. The expressions of the same four miRNAs as presented above in the BMP4 (4-day) treated human EPSCs and human ESCs. The choriocarcinoma cells JEG-3 that are representatives of extravillous trophoblasts and JAR that are representatives of villous trophoblast cells were used as the positive and negative control, respectively. **h**. DNA demethylation in the promoter region of the *ELF5* locus in cells differentiated from H1-EPSCs and other cells (6 days of SB431542 treatment). Cells from H1-ESCs, H1-naïve ESCs (5i) did not have substantial DNA demethylation at the *ELF5* promoter. **i**.

Secreted hormones from trophoblasts derived from H1-EPSCs induced by TGFβ inhibition (SB431542). VEGF, PLGF, sFlt-1and sEng were measured in the conditioned media of cells differentiated from EPSCs or ESC cultures upon SB431542 treatment over a 48h interval until day 16. **j**. hCG secreted from trophoblasts from EPSCs or ESCs. hCG secreted from day-10 differentiated (SB431542 treatment) EPSCs and ESCs were measured by ELISA. *P < 0.05 compared with H1-ESC. Data are mean ± s.d. (n = 3).

**Extended Data Figure 11**. Derivation and characterisation of TS cells from human and pig EPSCs. **a**. RT-qPCR analysis of pluripotency and trophoblast stem cell genes in four EPSC-derived TSC lines and their parental hEPSCs. **b**. Phase-contrast and Hoechst staining images of multinucleated syncytiotrophoblasts differentiated from TSCs. **c**. Detection of CGB in syncytiotrophoblasts differentiated from EPSC-TSCs. **d**. RT-qPCR analysis of trophoblast genes in three TSC lines and their derivative syncytiotrophoblast (ST) and extravillous trophoblast (EVT). **e**. Detection of HLA class I by monoclone antibody W6/32 in undifferentiated hESCs, hEPSCs, hTSCs, and in hEVT differentiated from hTSCs. Compared to hESCs, hEPSCs and hTSCs expressed substantially lower levels of HLA class I molecules. EVTs are known to express HLA-C. The choriocarcinoma cells JEG-3 and JAR are representatives of extravillous and villous trophoblast cells, respectively. JEG-3 express HLA-G and HLA-C and HLA-E, whereas JAR cells do not express any HLA molecules (Apps, R., et al. Immunology 2009). They were used as the positive and negative control, respectively. **f**. H3K27me3 and H3K4me3 marks at the loci encoding factors associated with placenta development in pig $EPSC^{Emb}$ and human H1-EPSCs. **g**. Images of primary TSC colonies (left) formed from individual pig $pEPSC^{Emb}$ on day 7 cultured in human TSC condition, and of TSCs at passage 7 (right) derived from

pEPSC$^{Emb}$. **h**. Expression of trophoblast factors GATA3 and KRT7 in pEPSC$^{Emb}$-TSCs detected by immunostaining. Nuclei were stained with DAPI. **h**. RT-qPCR analysis of pluripotency and trophoblast stem cells genes in four pEPSC$^{Emb}$-derived TSC-like lines and their parental pEPSC$^{Emb}$. Relative expression levels, normalized to *GAPDH*, were compared with those of the parental pEPSC$^{Emb}$ cells. Data are mean ± s.d. (n = 3).

**Extended Data Figure 12**. The effects of inactivation of *PARG* in human EPSCs on trophoblast differentiation potential. **a**. CRISPR/Cas9 mediated deletion of ~350bp in exon 4 of the *PARG* gene in the *CDX2-H2BVenus* reporter hEPSCs. Two gRNAs (g1, g2) were designed to target the largest coding exon. After transfection and selection, 6 clones out 48 clones were identified as bi-allelic mutants by PCR genotyping and were confirmed by sequencing. **b**. The CDX2-reporter EPSC cells with or without the *PARG* deletion were treated with the TGFβ inhibitor SB431542 for four days for trophoblast differentiation. The cells were analysed by flow cytometry. The percentages of Venus$^{+}$ cells indicate the extent of trophoblast differentiation of the parental cells. Inactivation of PARP caused decreased Venus$^{+}$ cells. Similar results were obtained in experiments using two independent *PARP*-deficient hEPSC lines. **c-e**. RT-qPCR analysis of expression of trophoblast genes in cells differentiated from either the control (wild type) or the *PARG-deficient CDX2-H2BVenus* H1-EPSCs, after 6 days of SB431542 treatment. Significantly lower trophoblast gene expression was found in the *PARG-deficient* cells. *$p < 0.05$. Data are mean ± s.d. (n = 3). Experiments were repeated at least three times.

# Figure 1

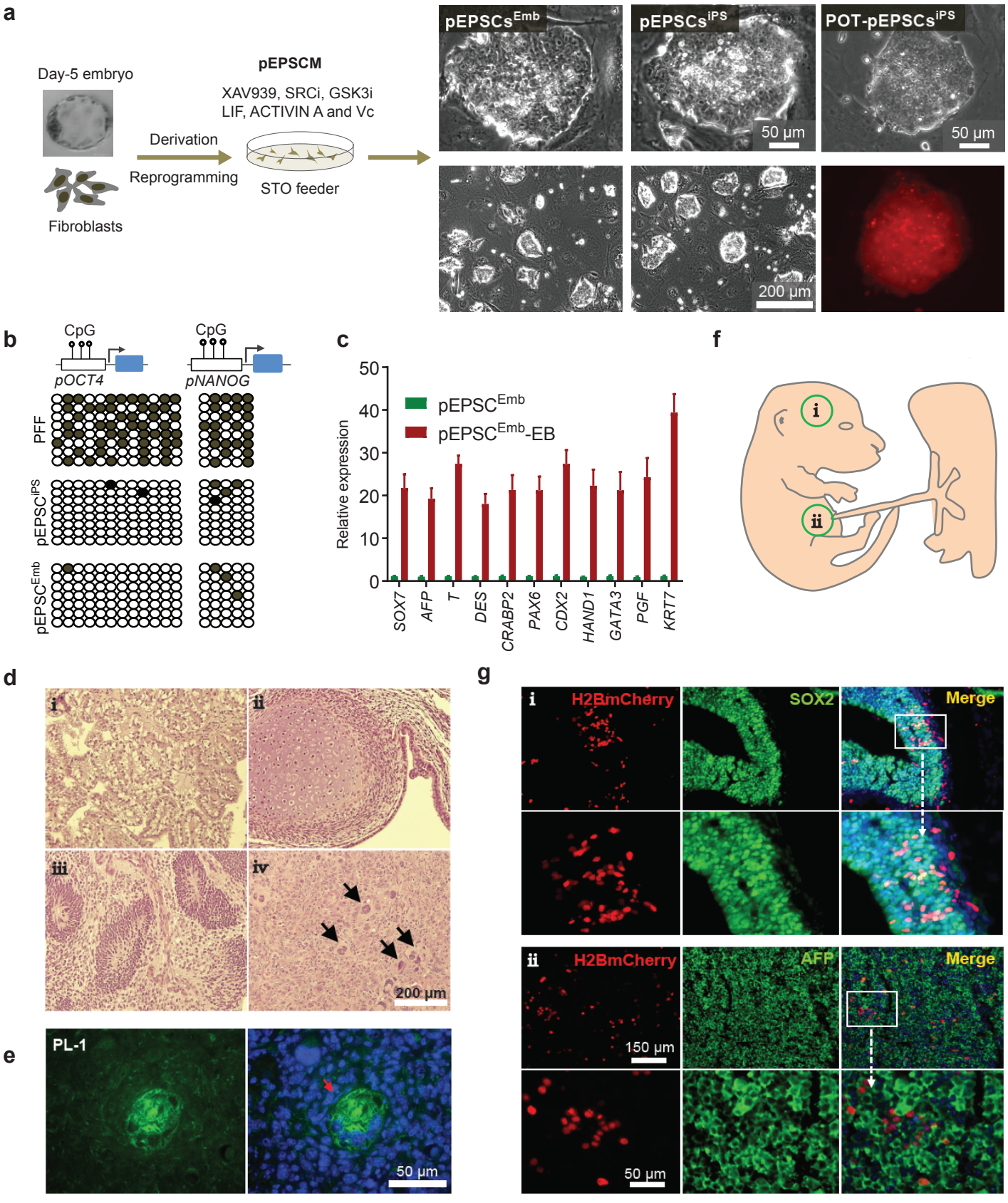
a
Day-5 embryo
pEPSCM
XAV939, SRCi, GSK3i
LIF, ACTIVIN A and Vc
Derivation
Reprogramming
STO feeder
Fibroblasts
pEPSCs^Emb
pEPSCs^iPS
POT-pEPSCs^iPS
50 μm
200 μm
b
CpG
CpG
pOCT4
pNANOG
PFF
pEPSC^iPS
pEPSC^Emb
c
Relative expression
pEPSC^Emb
pEPSC^Emb-EB
SOX7
AFP
T
DES
CRABP2
PAX6
CDX2
HAND1
GATA3
PGF
KRT7
f
i
ii
d
i
ii
iii
iv
200 μm
e
PL-1
50 μm
g
i
H2BmCherry
SOX2
Merge
ii
H2BmCherry
AFP
Merge
150 μm
50 μm

# Figure 2

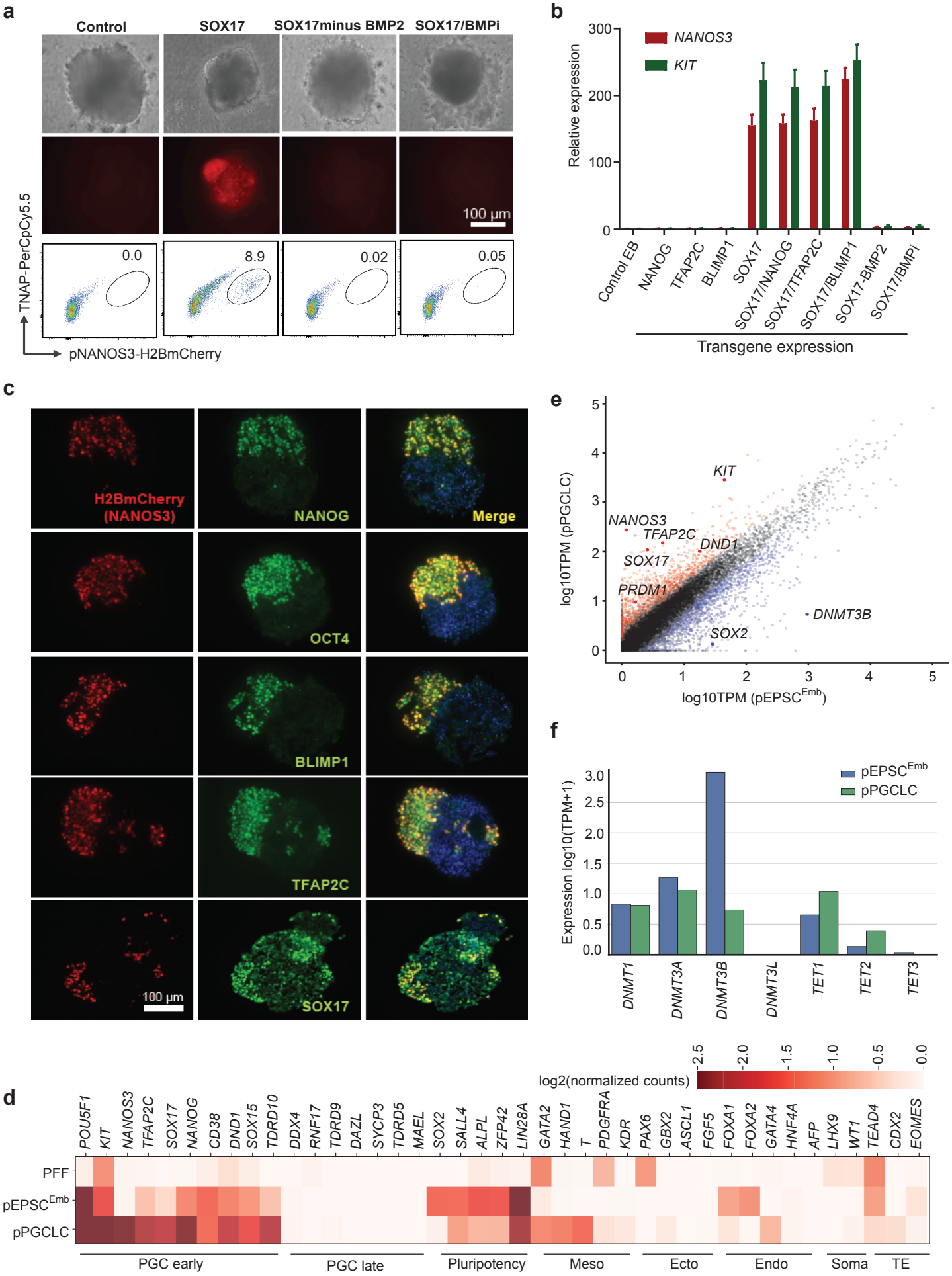
a
Control
SOX17
SOX17minus BMP2
SOX17/BMPi
100 µm
0.0
8.9
0.02
0.05
TNAP-PerCpCy5.5
pNANOS3-H2BmCherry
b
NANOS3
KIT
Relative expression
300
200
100
0
Control EB
NANOG
TFAP2C
BLIMP1
SOX17
SOX17/NANOG
SOX17/TFAP2C
SOX17/BLIMP1
SOX17-BMP2
SOX17/BMPi
Transgene expression
c
H2BmCherry (NANOS3)
NANOG
Merge
OCT4
BLIMP1
TFAP2C
SOX17
100 µm
e
KIT
NANOS3
TFAP2C
DND1
SOX17
PRDM1
DNMT3B
SOX2
log10TPM (pPGCLC)
log10TPM (pEPSC^Emb)
f
pEPSC^Emb
pPGCLC
Expression log10(TPM+1)
DNMT1
DNMT3A
DNMT3B
DNMT3L
TET1
TET2
TET3
d
log2(normalized counts)
POU5F1
KIT
NANOS3
TFAP2C
SOX17
NANOG
CD38
DND1
SOX15
TDRD10
DDX4
RNF17
TDRD9
DAZL
SYCP3
TDRD5
MAEL
SOX2
SALL4
ALPL
ZFP42
LIN28A
GATA2
HAND1
T
PDGFRA
KDR
PAX6
GBX2
ASCL1
FGF5
FOXA1
FOXA2
GATA4
HNF4A
AFP
LHX9
WT1
TEAD4
CDX2
EOMES
PFF
pEPSC^Emb
pPGCLC
PGC early
PGC late
Pluripotency
Meso
Ecto
Endo
Soma
TE

# Figure 3

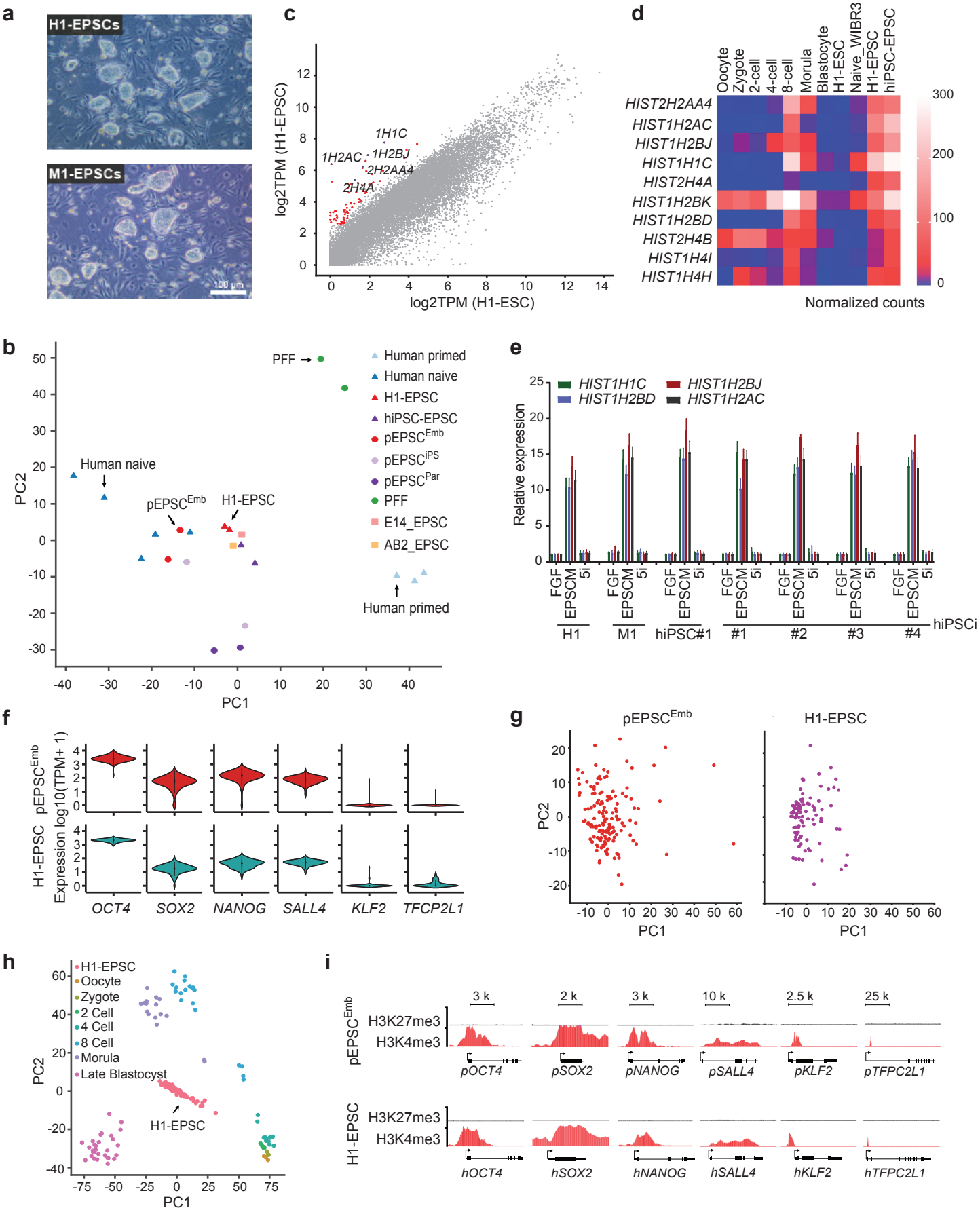
a
H1-EPSCs
M1-EPSCs
100 µm
c
log2TPM (H1-EPSC)
log2TPM (H1-ESC)
1H1C
1H2AC
1H2BJ
2H2AA4
2H4A
d
Oocyte
Zygote
2-cell
4-cell
8-cell
Morula
Blastocyte
H1-ESC
Naive_WIBR3
H1-EPSC
hiPSC-EPSC
HIST2H2AA4
HIST1H2AC
HIST1H2BJ
HIST1H1C
HIST2H4A
HIST1H2BK
HIST1H2BD
HIST2H4B
HIST1H4I
HIST1H4H
Normalized counts
b
PFF
Human primed
Human naive
H1-EPSC
hiPSC-EPSC
pEPSC^Emb
pEPSC^iPS
pEPSC^Par
PFF
E14_EPSC
AB2_EPSC
Human naive
pEPSC^Emb
H1-EPSC
Human primed
PC2
PC1
e
HIST1H1C
HIST1H2BJ
HIST1H2BD
HIST1H2AC
Relative expression
FGF
EPSCM
5i
H1
M1
hiPSC#1
#1
#2
#3
#4
hiPSCi
f
pEPSC^Emb
H1-EPSC
Expression log10(TPM+ 1)
OCT4
SOX2
NANOG
SALL4
KLF2
TFCP2L1
g
pEPSC^Emb
H1-EPSC
PC2
PC1
h
H1-EPSC
Oocyte
Zygote
2 Cell
4 Cell
8 Cell
Morula
Late Blastocyst
H1-EPSC
PC2
PC1
i
pEPSC^Emb
H1-EPSC
H3K27me3
H3K4me3
3 k
2 k
3 k
10 k
2.5 k
25 k
pOCT4
pSOX2
pNANOG
pSALL4
pKLF2
pTFPC2L1
hOCT4
hSOX2
hNANOG
hSALL4
hKLF2
hTFPC2L1

# Figure 4

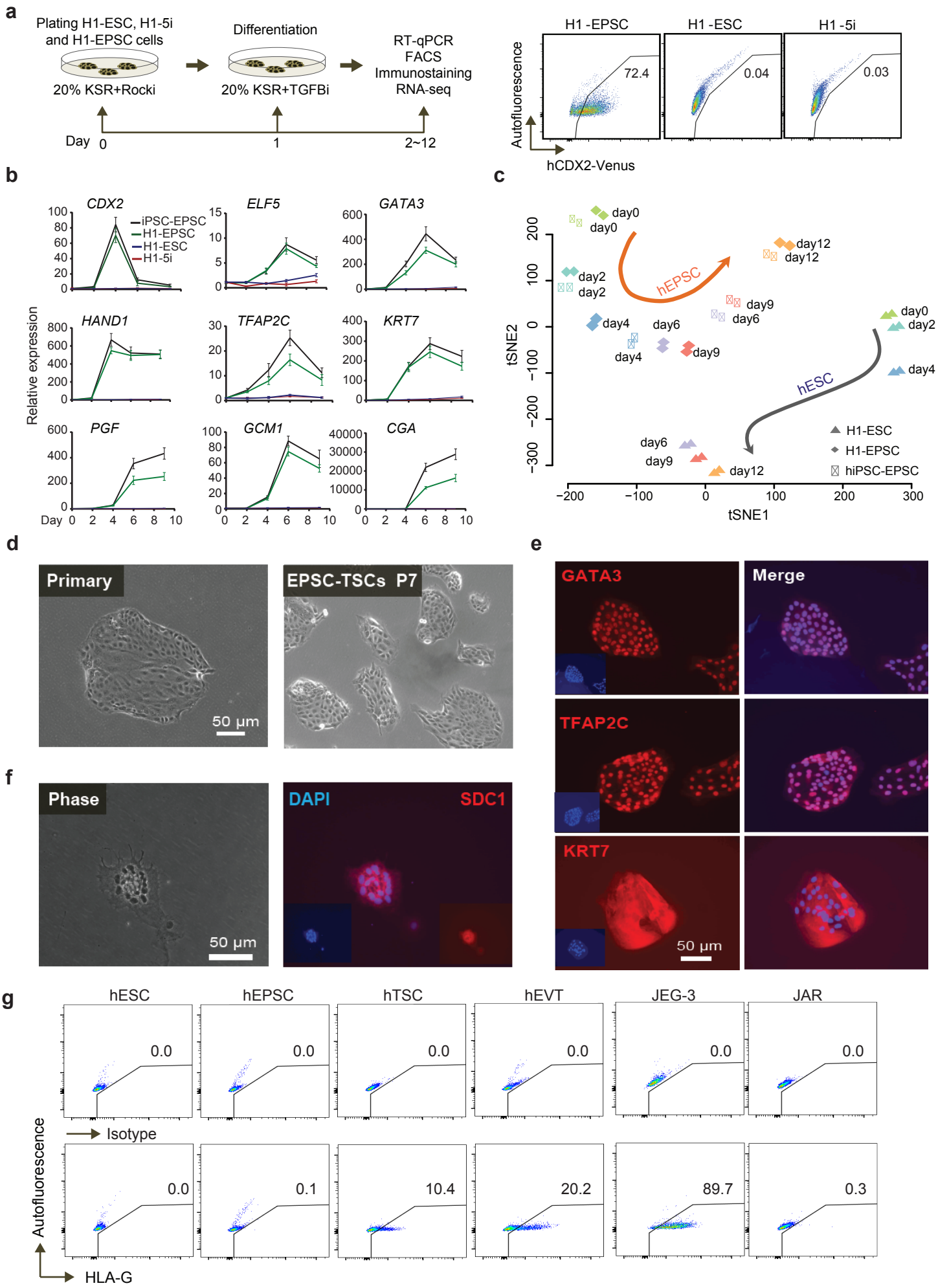
a
Plating H1-ESC, H1-5i and H1-EPSC cells
20% KSR+Rocki
Differentiation
20% KSR+TGFBi
RT-qPCR
FACS
Immunostaining
RNA-seq
Day 0
1
2~12
H1 -EPSC
H1 -ESC
H1 -5i
72.4
0.04
0.03
Autofluorescence
hCDX2-Venus
b
CDX2
ELF5
GATA3
HAND1
TFAP2C
KRT7
PGF
GCM1
CGA
iPSC-EPSC
H1-EPSC
H1-ESC
H1-5i
Relative expression
Day 0 2 4 6 8 10
c
day0
day2
day4
day6
day9
day12
hEPSC
hESC
H1-ESC
H1-EPSC
hiPSC-EPSC
tSNE1
tSNE2
d
Primary
EPSC-TSCs P7
50 μm
e
GATA3
Merge
TFAP2C
KRT7
50 μm
f
Phase
DAPI
SDC1
50 μm
g
hESC
hEPSC
hTSC
hEVT
JEG-3
JAR
0.0
Isotype
0.1
10.4
20.2
89.7
0.3
Autofluorescence
HLA-G

Table 1. Derivation of pEPSCs from preimplantation embryos

| Embryo origins | No. of blastocyst | No. (%) of outgrowth | No. (%) of cell lines |
|---|---|---|---|
| Parthenogenetic | 252 | 24 (10) | 12 (50) |
| *In vivo* derived | 76 | 27 (36) | 26 (96.3) |